

SUPPLEMENTARY INFORMATION FOR:
Towards effective carbon accounting for the global steel industry
within the EU carbon border adjustment mechanism

Tom Terlouw^{1,2*}, Carina Harpprecht^{3,4}, and Christian Bauer¹

Affiliations

¹ Laboratory for Energy Systems Analysis, PSI Centers for Nuclear Engineering and Sciences and for Energy and Environmental Sciences, Paul Scherrer Institute, 5232 Villigen PSI, Switzerland

² Chair of Energy Systems Analysis, Institute of Energy and Process Engineering, ETH Zurich, Zurich 8092, Switzerland

³ Leiden University, Institute of Environmental Sciences (CML), P.O. Box 9518, 2300 RA, Leiden, the Netherlands

⁴ German Aerospace Center (DLR), Institute of Networked Energy Systems, Curiestr. 4, 70563, Stuttgart, Germany

* Corresponding author: tom.terlouw@psi.ch.

Contents

Supplementary Note 1. Assumptions used for prospective scenarios for 2040	2
Supplementary Note 2. Additional results	4
SUPPLEMENTARY REFERENCES	9

Supplementary Note 1. Assumptions used for prospective scenarios for 2040

Here, we report the procedure used to design the future scenarios for 2040. For those two scenarios, the following generic assumptions are used:

- All steel production facilities (after construction year 1950) defined as ‘*operation*’, ‘*announced*’, ‘*Finalized (research & testing)*’, and ‘*construction*’ in the following databases are included:
 - Global steel plant tracker¹
 - Green steel tracker²
- It is based on the IMAGE scenario (2°C pathway, SSP2-RCP2.6)³, where global crude steel demand is projected to reach 2150 Mt/year by 2040.
- With the following production mix (2°C pathway, SSP2-RCP2.6)³:
 - 67% primary steel
 - 33% secondary steel
- Even after accounting for all available steel production plants in the two databases used, a deficit of more than 800 Mt/year remains compared to the IMAGE scenario. Thus, a generic multiplication factor (specific for primary and secondary steel) is applied to meet the target production of almost 2150 Mt/year.

However, for the two different scenarios, the following assumptions are used based on the specific pathway.

Scenario (i): primary steel production via BF-BOF with CCS

- Primary steel production processes are substituted by using BF-BOF (blast furnace–basic oxygen furnace) with carbon capture and storage (CCS).
- Exceptions:
 - Primary steel produced via EAF-DRI using hydrogen is left as is.

Scenario (ii): primary steel production via EAF-DRI using hydrogen

- Primary steel production processes are substituted by using EAF-DRI (electric arc furnace–direct reduced iron) with hydrogen as the reducing agent.
- Exceptions:
 - Primary steel via BF-BOF with CCS is left as is.

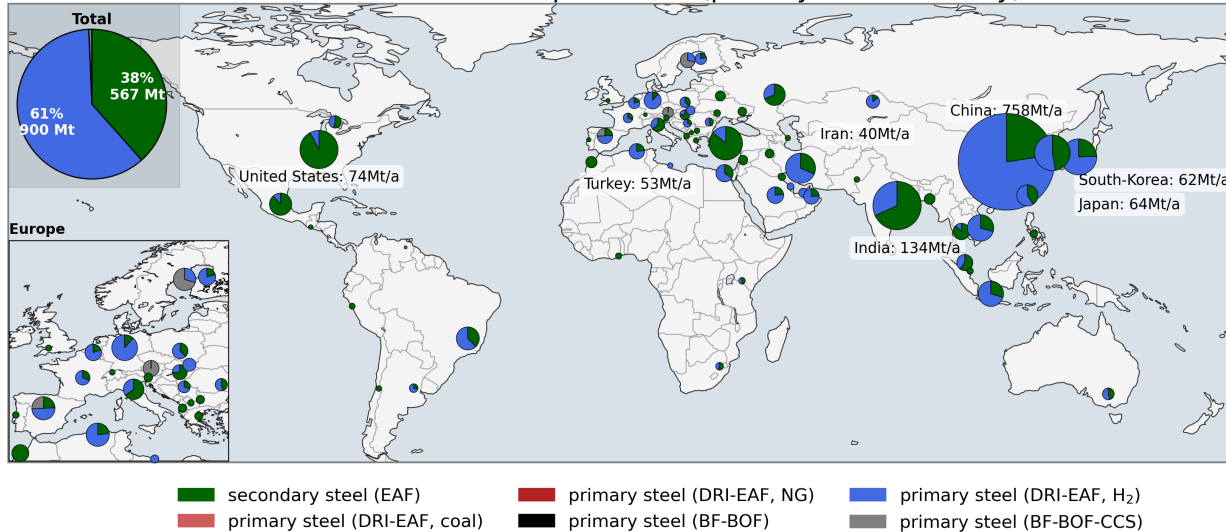
We follow a similar approach using another IAM, the one from REMIND aimed at limiting global warming to 2°C (SSP2-PkBudg1150)^{4,5}. Here, global crude steel demand is projected to reach 1686 Mt/year by 2040.

Supplementary Note 2. Additional results

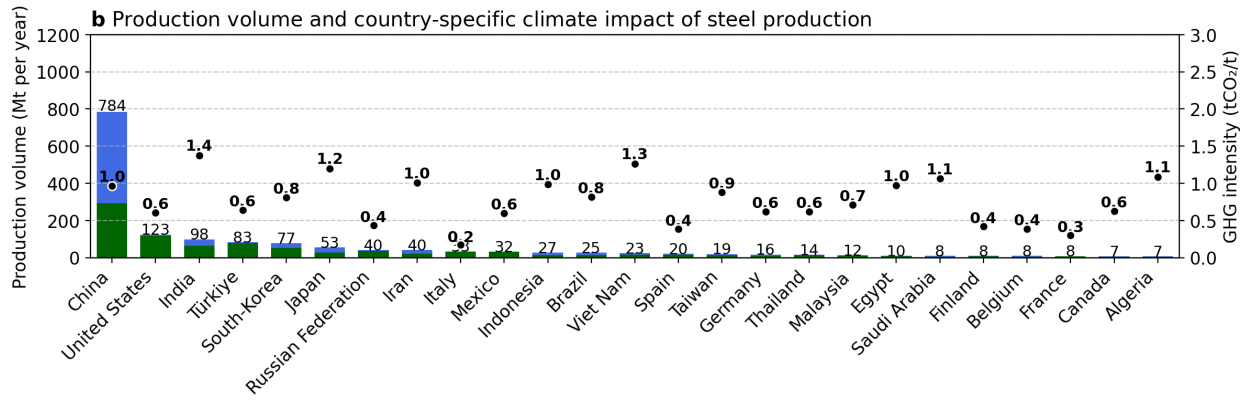
Additional results: REMIND

Supplementary Figures 1–6 provides additional results for another IAM; REMIND^{4,5}. Those supplementary figures are logically only created for the future scenario for 2040, considering the scenarios mainly producing steel via (i) H₂-DRI-EAF (Supplementary Figures 1–3) and (ii) BF-BOF with carbon capture and storage (BF-BOF-CCS) (Supplementary Figures 4–6). Note that those results are modified to be representative of the steel demand in the REMIND 2 °C pathway by applying a demand of 1686 Mt steel per year.

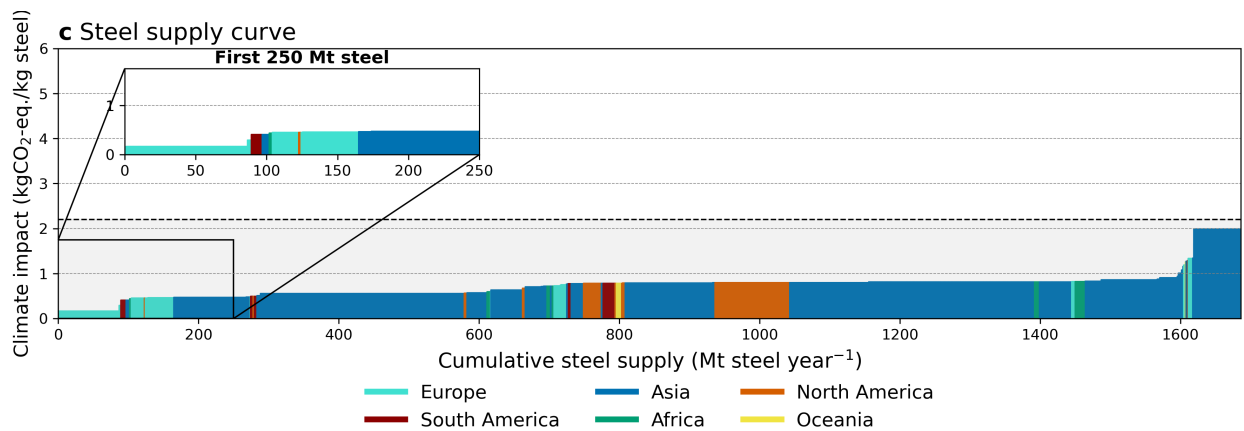
a Global GHG emissions from crude steel production (primary and secondary)



Supplementary Figure 1: Annual global greenhouse gas emissions from steel production in 2040 under the hydrogen-based pathway, as modeled in REMIND. The figure highlights total emissions across different production technologies and regions.

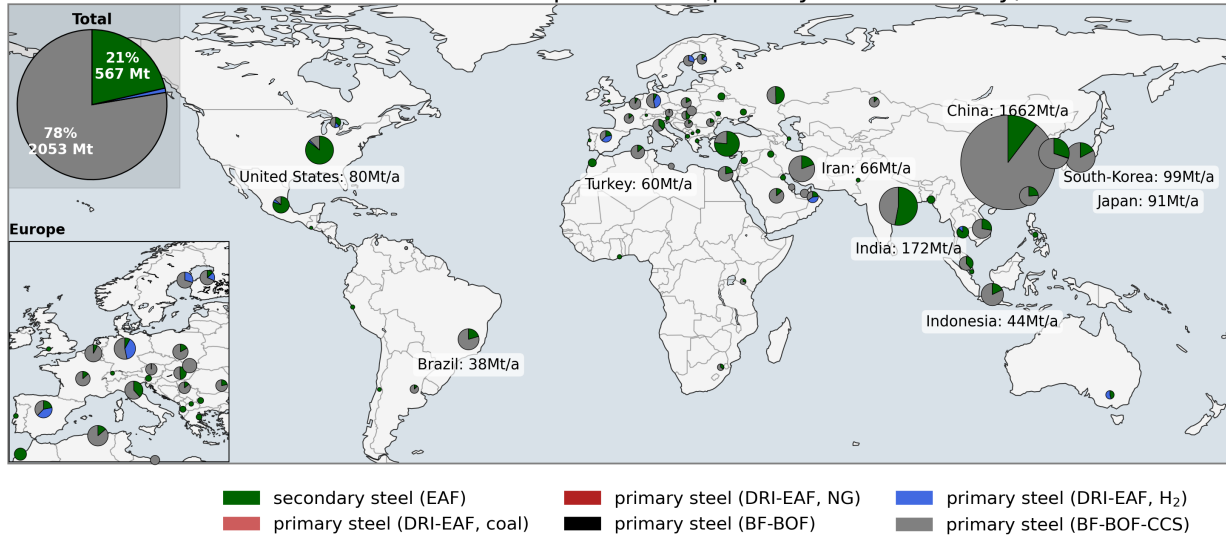


Supplementary Figure 2: GHG intensity (averaged GHG emissions per ton of steel) for various countries, the hydrogen-based scenario in REMIND. The figure illustrates differences in emissions efficiency across technologies and regions.

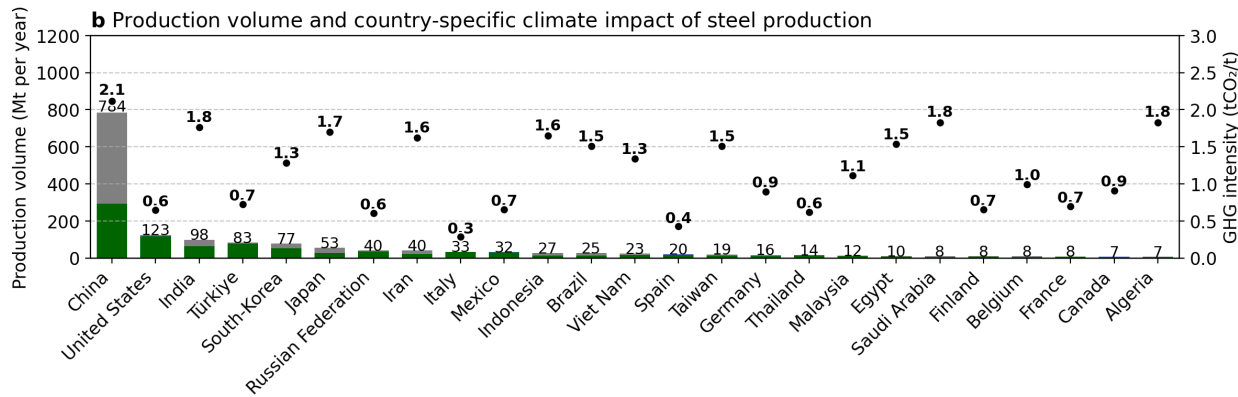


Supplementary Figure 3: Steel supply curve for 2040 under the hydrogen-based production scenario in REMIND. The curve illustrates GHG emissions per unit of steel as cumulative steel production volumes increase.

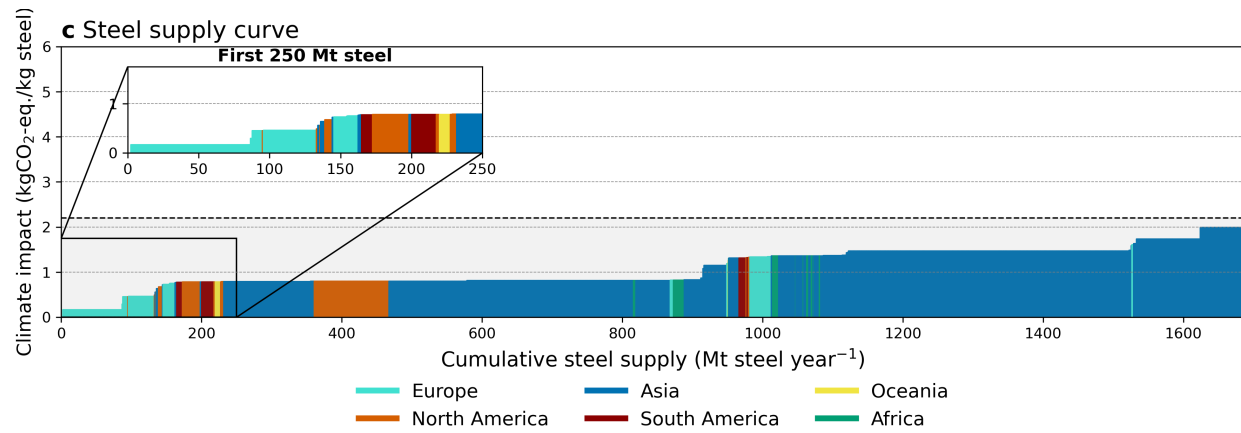
a Global GHG emissions from crude steel production (primary and secondary)



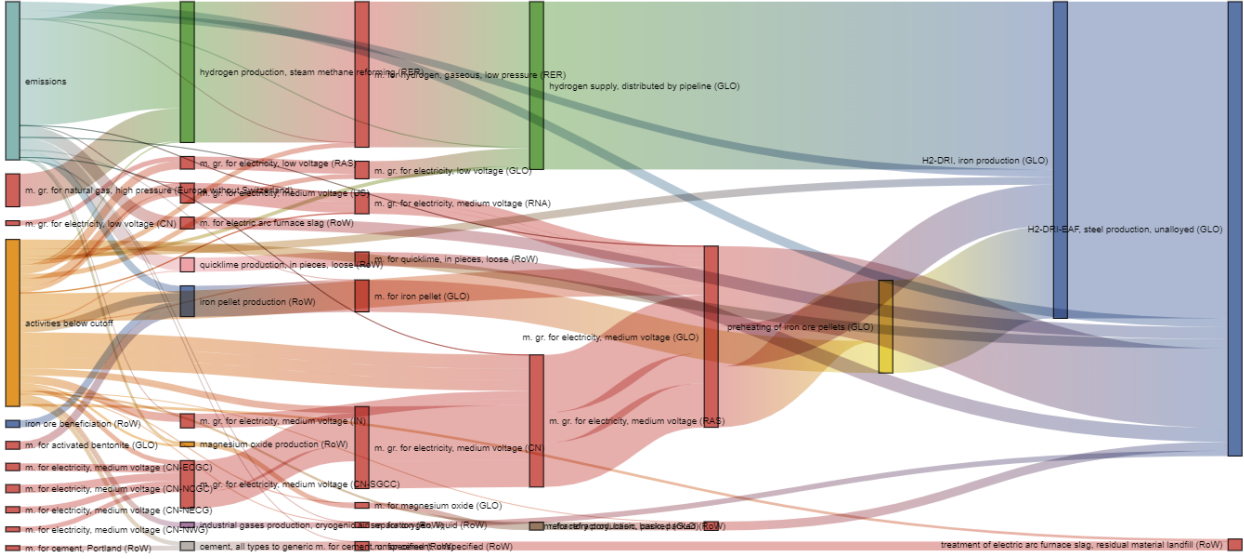
Supplementary Figure 4: Annual global greenhouse gas emissions from steel production in 2040 under the BF-BOF-CCS pathway, as modeled in REMIND. The figure highlights total emissions across different production technologies and regions.



Supplementary Figure 5: GHG intensity (averaged GHG emissions per ton of steel) for various countries, the BF-BOF-CCS scenario in REMIND. The figure illustrates differences in emissions efficiency across technologies and regions.



Supplementary Figure 6: Steel supply curve for 2040 under the BF-BOF-CCS production scenario in REMIND. The curve illustrates GHG emissions per unit of steel as cumulative steel production volumes increase.



Supplementary Figure 7: Illustrative Sankey diagram for steel production via hydrogen-based direct reduced iron (H₂-DRI) combined with an electric arc furnace (EAF), highlighting the main contributors to climate change impacts along the value chain. The diagram shows how upstream supply chain processes contribute to the overall emissions of this pathway. Interactive Sankey diagrams for all hydrogen-based steel production pathways are available as HTML files in the online repository.

Sankey diagrams of steel production pathways considered in Figure 4 of the paper

To offer a clearer understanding of the main GHG emission contributions throughout different steel production pathways presented in Figure 4 of the manuscript, we have created Sankey diagrams for each steel production pathway for three scenarios: the current one, year 2040 using the REMIND 2°C scenario, and year 2040 utilising the IMAGE 2°C scenario.

These diagrams are provided as interactive HTML files and are available in the accompanying online GitHub repository. Here, we present a single illustrative example (Supplementary Figure 7), while the complete set of Sankey diagrams for all hydrogen applications can be accessed through the repository.

The example shown includes five levels of steel production via the H₂-DRI-EAF route for the current scenario. The primary contributors to climate change impacts in this case are iron production (and especially the hydrogen supply mix) and iron pellets. As users move from right to left in the Sankey diagram, they can explore increasingly granular contributions from upstream processes, illustrating how embedded climate impacts accumulate throughout the supply chain. The interactive HTML format allows users to hover over individual flows to examine the specific impacts of each supply chain activity in detail.

SUPPLEMENTARY REFERENCES

1. Monitor, G. E. *Global Steel Plant Tracker* Apr. 2024. <https://globalenergymonitor.org/projects/global-steel-plant-tracker/>.
2. For Industry Transition, L. G. *Green Steel Tracker* 2024. <https://www.industrytransition.org/green-steel-tracker/>.
3. Vuuren, D. V., Stehfest, E. & Gernaat, D. THE 2021 SSP SCENARIOS OF THE IMAGE 3.2 MODEL Oktober 2021. <https://doi.org/10.31223/X5CG92> (2021).
4. Baumstark, L. *et al.* REMIND2.1: Transformation and innovation dynamics of the energy-economic system within climate and sustainability limits. *Geoscientific Model Development Discussions*, 1–50 (2021).
5. Luderer, Gunnar and Leimbach, Marian and Bauer, Nico and Kriegler, Elmar and Baumstark, Lavinia and Bertram, Christoph and Giannousakis, Anastasis and Hilaire, Jerome and Klein, David and Levesque, Antoine and Mouratiadou, Ioanna and Pehl, Michaja and Pietzcker, Robert and Piontek, Franziska and Roming, Niklas and Schultes, Anselm and Schwanitz, Valeria Jana and Strefler, Jessica. *Description of the REMIND model (Version 1.6)* 2015. <https://ssrn.com/abstract=2697070>.